Low Temperature Properties of Acetonitrile Confined in MCM-41

Shigeharu Kittaka,* Takafumi Iwashita, Akihiro Serizawa, Miki Kranishi, and Shuichi Takahara

Department of Chemistry, Faculty of Science, Okayama University of Science, 1−1 Ridaicho, Okayama 700-0005, Japan

Yasushige Kuroda and Toshinori Mori

Department of Chemistry, Faculty of Science, Okayama University, Tsushima, Okayama 700-8530, Japan

Toshio Yamaguchi

Advanced Materials Institute and Department of Chemistry, Faculty of Science, Fukuoka University, Nanakuma, Jyonan-ku, Fukuoka 814-0180, Japan

Received: May 11, 2005; In Final Form: October 15, 2005

The effect of confinement on the phase changes and dynamics of acetonitrile in mesoporous MCM-41 was studied by use of adsorption, FT-IR, DSC, and quasi-elastic neutron scattering (QENS) measurements. Acetonitrile molecules in a monolayer interact strongly with surface hydroxyls to be registered and perturb the triple bond in the C≡N group. Adsorbed molecules above the monolayer through to the central part of the cylindrical pores are capillary condensed molecules (cc-acetonitrile), but they do not show the hysteresis loop in adsorption−desorption isotherms, i.e., second order capillary condensation. FT-IR measurements indicated that the condensed phase is very similar to the bulk liquid. The cc-acetonitrile freezes at temperatures that depend on the pore size of the MCM-41 down to 29.1 Å (C14), below which it is not frozen. In addition, phase changes between α-type and β-type acetonitriles were observed below the melting points. Application of the Gibbs−Thomson equation, assuming the unfrozen layer thickness to be 0.7 nm, gave the interface free energy differences between the interfaces, i.e., $\Delta\gamma_{l/\alpha} = 22.4$ mJ m^{-2} for the liquid/pore surface (ps) and α-type/ps, and $\Delta\gamma_{\alpha/\beta} = 3.17$ mJ m^{-2} for α-type/ps and β-type/ps, respectively. QENS experiments substantiate the differing behaviors of monolayer acetonitrile and cc-acetonitrile. The monolayer acetonitrile molecules are anchored so as not to translate. The two Lorentzian analysis of QENS spectra for cc-acetonitriles showed translational motion but markedly slowed. However, the activation energy for cc-acetonitrile in MCM-41 (C18) is 7.0 kJ mol^{-1} compared to the bulk value of 12.7 kJ mol^{-1}. The relaxation times for tumbling rotational diffusion of cc-acetonitrile are similar to bulk values.

Introduction

The physicochemical properties of fluids in a confined geometry are among the most important subjects to study from both fundamental and practical perspectives.[1] Accordingly, a number of experimental and theoretical works have been conducted on many systems, such as catalysts, biological systems, soils, etc.[1−6] Until the beginning of the 1990s, except for zeolites that just have micropores, porous materials had not been homogeneous in pore size and shape, although there have been a number of models of pore structures and calculations on them.[1,7,8] Accordingly, the results obtained have not yet led to a concrete understanding of the physicochemical phenomena of fluids in a confined geometry. The succeeding development of new porous materials FSM,[9] MCM-41S,[10] and SBA,[11] which started at the beginning of the 1990s, resulted in a great breakthrough in understanding the fundamental and important problems, not only for surface science but also for materials science. Some of these materials take the honeycomb structures of mesopores, i.e., cylinders ranging from 2−10 nm in diameter.[10,12] At present, highly desired but lacking are homogeneous porous materials with pores larger than 10 nm. Thus, there is still much work using porous glasses like Vycol and cpg (controlled porous glass) that have relatively narrow pore size distributions but are heterogeneous, because there are many systems involving such large pores, e.g., cements, oil shale, biological cells, and materials for practical use.[13−16]

Among many molecules, water is one of the commonest molecules present in various kinds of porous systems. Accordingly, there has been much work reported with these well-defined porous silicas since their development.[17−25] When studying these systems, however, the originally developed MCM-41 and FSM are degraded quickly by contact with saturated water vapor and/or liquid water.[21,26] This is due to the contaminant Na ions that have been unavoidably included in the formation. This problem was successfully solved by decreasing them before removing the organic templates by heating.[28] Thus, refined MCM-41 samples should permit a precise study of the confinement effect on the physicochemical behavior of aqueous fluids.

Work before the 1990s has been successfully found to obey a general rule describing the phase changes, representatively

* Author for correspondence. E-mail: kittaka@chem.ous.ac.jp. Telephone: +81-86-256-9433. Fax: +81-86-256-9757.

10.1021/jp052476g CCC: $30.25
Published on Web 11/17/2005

solid−liquid, namely the Gibbs−Thomson (G−T) relation.[29−31] Because of the simplicity of the G−T equation due to arbitrary conditioning of the system, which should be noted afterward, and of the less well-defined character of the pores, it has not been possible to define the character of the fluids in the porous systems clearly.[32] Thus, much effort using well-defined porous materials has been expended for these objectives.

Acetonitrile is an aprotic polar molecule and used in many areas as a solvent, e.g., analytical chemistry, inorganic and/or organic syntheses, chromatography, etc. It is very useful as a developing solvent for chromatography, where the solution must pass through the pore matrices of the packed bed. That is, chemical processes of the solution occur in the confined geometry of channels of the packing for which the fluid property should be taken into account. On the other hand, acetonitrile is a good probe to research the surface acidity of metal oxide catalysts,[33] in which interactions with the solid surface are involved. However, there has not been much work on this subject. Thus, the physicochemical properties of this molecule in porous silica, which has an acidic surface, should permit the understanding of a typical model of molecules in a confined geometry. Recently, new porosiometries using H NMR[34] and Xe−NMR[35] were proposed by filling acetonitrile in porous silicas. However, acetonitrile takes two crystalline forms, a monoclinic α-type[36] and an orthorhombic β-type;[37] the former transforms into the latter at decreasing temperatures and vice versa just below the melting point (mp, 229.315 K; tp, 216.9 K).[38] This transition temperature is not very far from the melting point and thus cannot be ignored in the analysis of pore size distribution. However, the authors in refs 31 and 32 did not include the phase transition in their analysis. It seems to be necessary to study the phase transitions of acetonitrile in the well-defined MCM-41 as an important model system of confinement.

This article is composed of two studies: (1) the phase properties of acetonitrile confined in the mesopores of MCM-41 having a well-hydroxylated surface and (2) its dynamic properties.

Experimental Section

Sample Preparation. The MCM-41 sample was prepared by the modified Beck method.[28] Long-chain alkyltrimethylammonium bromides were used as templates, $R-(CH_3)_3N^+Br$: $R = C_nH_{2n+1}$. MCM-41 samples were named C10 ($d = 2.04$ nm), C12 (2.38 nm), C14 (2.91 nm), C16 (3.11 nm), C18 (3.61 nm), and C22 (4.19 nm) according to the number of carbon atoms in the longest alkyl group, R, of the template molecules. The materials formed are all resistant to water contact, which was confirmed by repeated adsorptions of water molecules. Honeycomb structures of samples were confirmed by powder XRD and TEM observations; at least four XRD peaks were observed, and in the cases of C16 and C18, six and five peaks were found. All of the sample surfaces were hydrated by contacting with saturated water vapor after overnight evacuation using a turbo-molecular pump, and finally they were evacuated overnight at 298 K. The acetonitrile used was from Wako Pure Chemical Ind. Ltd. (purity 99.8%). It was dried by use of preheated molecular sieve 5A and distilled.

Measurements. *(1) Adsorption of Acetonitrile.* Acetonitrile was adsorbed into a 30 mg sample of hydroxylated MCM-41. In the range of capillary condensation, equilibration time was around 20 min. Before and after that range it was about 3 min. To test the effect of hydration on the adsorbability of acetonitrile, samples were preheated at 773 K for 4 h in a vacuum. Adsorption measurements were conducted automatically by use of Rubotherm (BEL Japan) linked with a personal computer. Vapor pressure was controlled also by a computer connected to an MKS Baratron capacitance manometer Type 390H and vacuum line.

(2) Fourier Transform Infrared (FT-IR) Absorption. Sample powder (2−3 mg) was pelleted under a pressure of 4.0 MPa to form a disk of diameter 12 mm. The sample disk was mounted in a cryostat that was composed of two coaxial chambers with quartz windows for each. In the former, the sample disk was held on a copper sample holder in the inner chamber. A space between the two cylindrical chambers was evacuated during the experiment for thermal insulation. To test the effect of surface hydroxyls on the adsorption of acetonitrile, MCM-41 (C14) sample was heated to 673 K in a vacuum for 1 h. That is lower than the temperature for adsorption measurements due to the highest temperature limit of the apparatus that was used. The low temperature of the sample was controlled with liquid N_2 and electrical heating. The temperature was controlled by ± 2 K. For FT-IR measurements, the sample was pretreated as in the adsorption measurements. Measurements were repeated several times at each vapor pressure of acetonitrile to attain the equilibrated spectrum. To avoid evaporation of acetonitrile from the pores the sample chamber was filled with 1 atm nitrogen after adsorption of acetonitrile by a programmed amount. The FT-IR apparatus used was a JEOL JIR-100. The resolution was 4 cm^{-1} and measurement was scanned for 100 repetitions.

(3) Differential Scanning Calorimetry. The phase change of acetonitrile was studied calorimetrically by the use of differential scanning calorimetry, DSC. Sample specimens were prepared as follows. Sample powder was hydrated with saturated water vapor after evacuation of the samples in a glass ampule of inner diameter 4 mm, followed by evacuation by turbo-molecular pump overnight and sealing to form an ampule with a long thin end (1 cm) so as to break in the liquid acetonitrile. This permits the introduction of acetonitrile directly into the pores without exposing the sample to air. The prepared wet sediment was transferred quickly into a sample aluminum cell and excess liquid was removed with filter paper until it looked dry. Finally, samples were sealed by use of a crimper. The sample was ca. 6 mg. Measurements were performed at a rate of 5 K min^{-1} for both cooling and heating of the systems. The DSC apparatus used was a DSC-Q10 manufactured by TA Instruments.

(4) Incoherent Quasi-Elastic Neutron Scattering (QENS) Measurements. By taking advantage of the high incoherent scattering cross section of protons to the neutron beam, the dynamic properties of acetonitrile molecules in the MCM-41 were studied by probing the motion of methyl group hydrogens with QENS measurements. The spectrometer used was AGNES (JAERI). The wavelength of the neutron beam was 4.22 Å. The MCM-41 samples were packed in the interstitial space of two coaxial aluminum cylinders and treated similarly to the above experiments: evacuation, hydration, evacuation, and adsorption of acetonitrile from the gas phase at the programmed pressures. Vapor pressure was controlled as follows: for C10 monolayer, relative pressure $P/P_0 = 0.052$; cc-C10, $P/P_0 = 0.461$; cc-C18, $P/P_0 = 0.739$. Samples were prepared so that the transmission was around 90%, to avoid multiple scattering. Acquisition of the data was performed for 10 h and the resolution function of the system was determined by a vanadium rod (half-width at half-maximum of the spectrum, HWHM = 80 μeV).

Results and Discussion

Interactions of Acetonitrile Molecules with the MCM-41 Surface. Figure 1 shows stepwise adsorption isotherms of

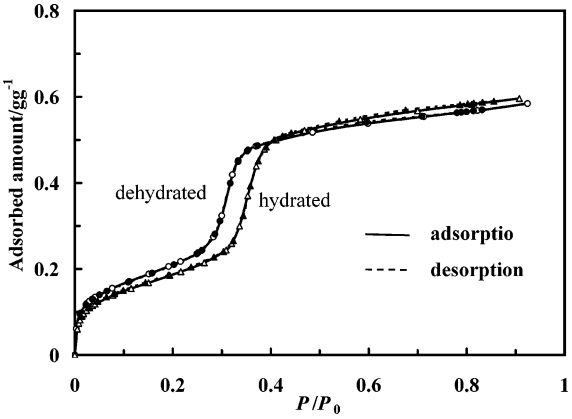

Figure 1. Effect of surface hydration on the adsorbability of acetonitrile into MCM-41 (C14) at 298 K. Hydrated: as-prepared C14 sample was evacuated overnight at 298 K and hydrated overnight in a saturated water vapor, followed by evacuation at 298 K. Dehydrated: hydrated sample is heated at 773 K under vacuum for 4 h.

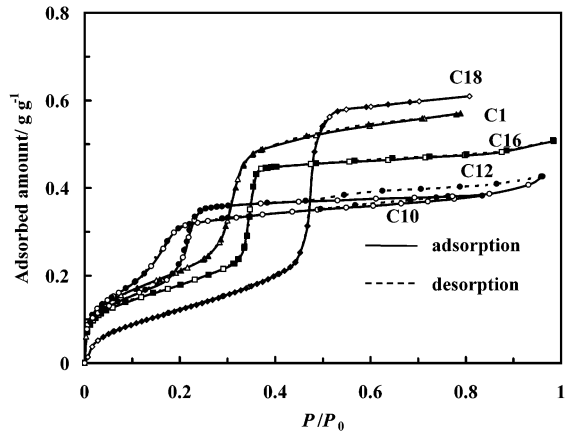

Figure 2. Adsorption isotherms of acetonitrile into MCM-41 varying in pore sizes. The pore sizes are 2.04 nm for C10, 2.91 nm for C14, and 3.61 nm for C18.

acetonitrile on the MCM-41 (C-14) samples hydrated and heated for 2 h in a vacuum at 773 K. Capillary condensation in the former occurs at a higher pressure than it does in the latter. The total adsorbed amounts after capillary condensation are similar for the two preparations, and in each system the desorption branch coincides with that for the adsorption branch (reversible adsorption). Thus, we can conclude that acetonitrile is adsorbed without chemical reaction or dissociative adsorption. In fact, however, the as-prepared sample is not hydrated fully in humid air ($P/P_0 \cong 0.7$) and is rather hydrophobic. Thus, samples were hydrated fully (ca. 2.7 OH nm^{-2}) by contacting with the saturated water vapor and evacuated. Figure 2 shows the adsorption isotherms of acetonitrile on the hydroxylated MCM-41 samples of various pore diameters (C10, C14, C16, and C18). One can clearly see the typical sequential change of isotherms, where capillary condensation appears at increasing pressures with pore size increase. Here, in all systems desorption isotherm runs on the adsorption isotherm and does not show hysteresis loop. This fact signifies that observed capillary condensation is an second-order process which occurs above the capillary critical temperature.[32,39] However, as discussed below, adsorbed phase can be identified as a liquid acetonitrile. Adsorption mechanism awaits the further adsorption experiments at wide temperatures range and will be reported in the future. Absolute amounts cannot be compared straightforwardly because the thickness of the pore wall differs depending upon the

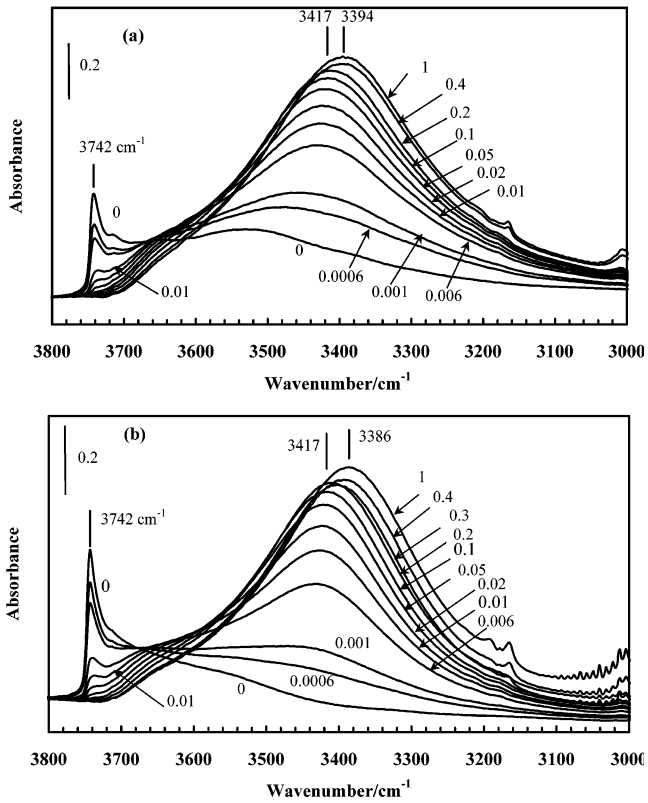

Figure 3. FT-IR spectra of surface hydroxyls affected by adsorption of acetonitrile into (a) C14 hydrated at 298 K and (b) C14 dehydrated at 673 K. Measurements were conducted at 298. The numbers 0−1 in the figure are relative pressures.

preparation batches of the sample. These isotherms were used for controlling the adsorbed amount of the samples for other experiments.

Fourier Transform Infrared (FT-IR) Absorption Spectra of Acetonitrile Adsorbed into MCM-41. Interactions of acetonitrile with surface hydroxyls on the pore surface of MCM-41 were analyzed by FT-IR spectroscopy. Phenomenologically, experimental results were common among all the MCM-41 samples varying in pore sizes. Examples of FT-IR spectral changes of stretching bands of hydroxyls are shown in Figure 3, parts a and b, as a function of vapor pressure for hydrated and heated (673 K) samples of MCM-41 (C14). It is clear that heat treatment of the samples diminishes the broad band around 3500 cm^{-1}, which is assigned to the various forms of hydroxyls, free and hydrogen bonded ones.[28] Instead, the 3742 cm^{-1} band for isolated surface hydroxyls became sharpened upon heating. This band was decreased markedly by dosing a small amount of acetonitrile. Its pressure range up to $P/P_0 = 0.01$ corresponds to adsorption up to the b-point of adsorption isotherm. It is interesting to note that the spectral change presents an isosbestic point in both samples, suggesting registered adsorptions of acetonitrile molecules on the isolated surface hydroxyls. Further adsorption should occur on the other hydroxyls and/or siloxane surface after the break of the isosbestic point. It is to be noted that the band shape changes just before capillary condensation at 3417−3394 cm^{-1}, suggesting perturbation of the surface hydroxyls by adsorption. After capillary condensation, the spectral change was quite small.

Figure 4a shows FT-IR spectra of acetonitriles adsorbed onto the C14 sample. Two bands appear at 2298 and 2264 cm^{-1} in the low-pressure range, the former of which is due to the combination band of C−C stretching and CH_3 symmetric bending modes and the latter to the stretching band of the

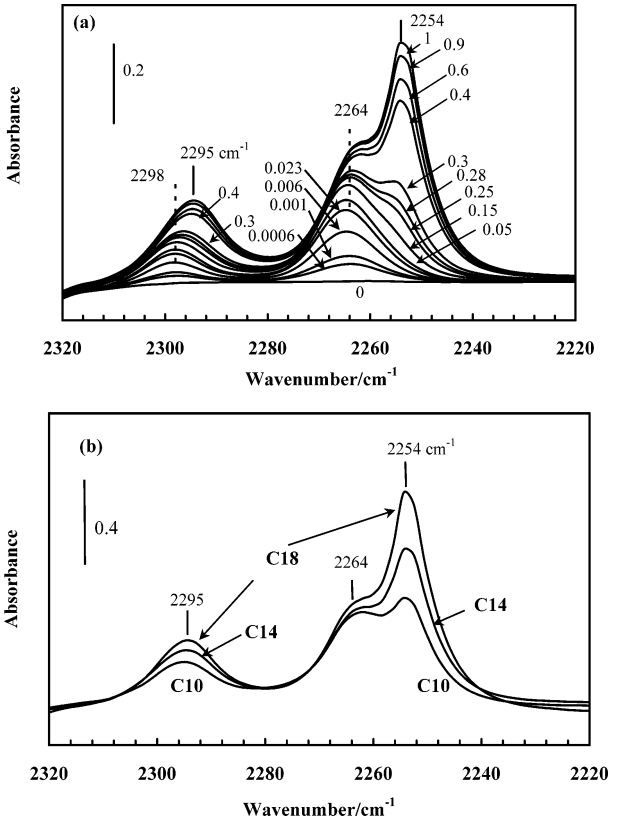

Figure 4. FT-IR spectra of (a) acetonitriles adsorbed into C14 hydrated at 298 K, where the numbers 0−1 in the figure are relative pressures, and (b) acetonitriles capillary condensed into hydrated MCM-41 samples (C10, C14, and C18) varying in pore sizes. Measurements were conducted at 298 K.

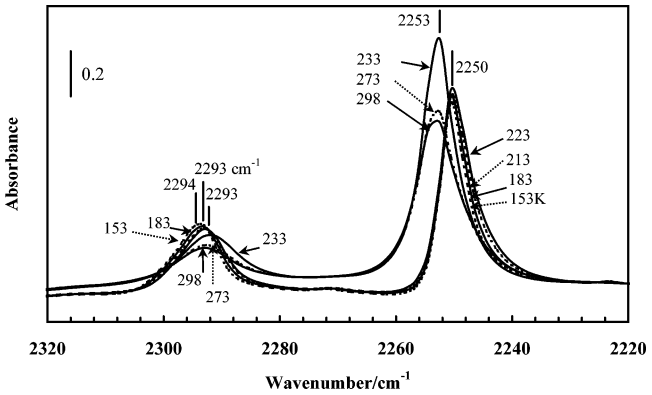

Figure 5. FT-IR spectra of bulk acetonitriles observed at increasing temperatures after freezing below 170 K. Liquid acetonitrile was sandwiched between the ZnSe crystal plates, a periphery of which was sealed with epoxy resin.

C≡N bond of acetonitrile coordinated to silanol groups, which are acidic sites.[33,40] The band intensity increased with pressure and the position remained unchanged. This area agrees completely with that of monolayer adsorption (Figure 3a), indicating that the adsorption occurs on the isolated surface hydroxyls.

With increase in the adsorbed amount of acetonitrile, a shoulder appears at lower wavenumbers and grows to give a band at 2254 cm^{-1}, which can be assigned to liquid acetonitrile (Figure 5). The spectral behaviors are similar to that reported by Tanaka et al.[37] A small displacement of the combination band at high pressures reflects the change in the adsorbed state of acetonitrile on the silica surface. Figure 4b compares clearly the spectra for the samples differing in pore size: the ratio of

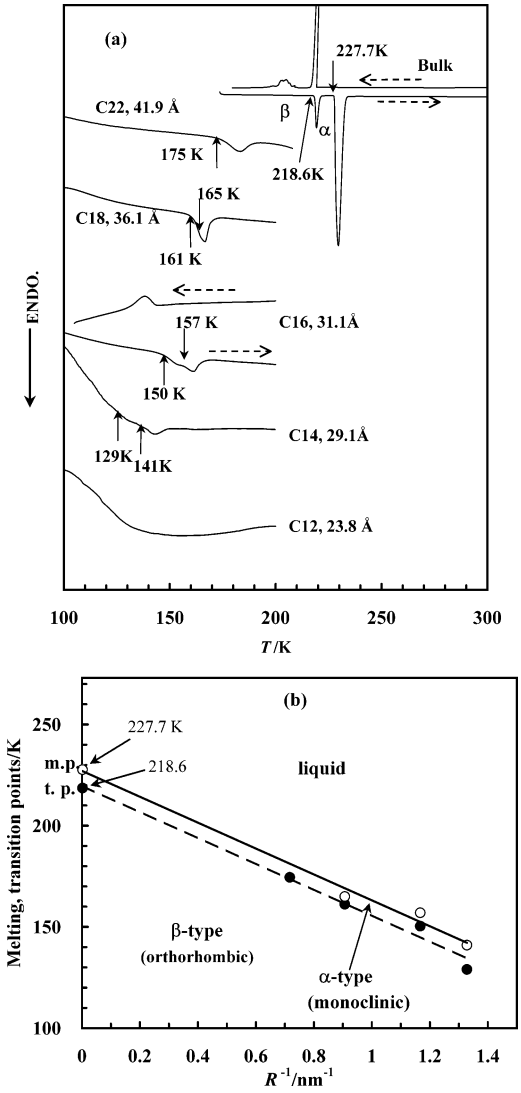

Figure 6. (a) DSC curves of acetonitriles condensed in the mesopores of MCM-41. Cooling and heating rates were 5 K min^{-1}. To visualize the profile clearly curves were multiplied arbitrarily. (b) Gibbs−Thomson plots of transition temperatures from β-phase to α-phase and melting points from α-phase to the liquid acetonitrile. Least-squares fitting was done so as to pass the intersection point for each phase change.

peak intensity of 2254 cm^{-1} in the C≡N vibration range increases with pore size.

Phase Changes with Temperature of Acetonitrile Confined in the Pores. Figure 6a shows the DSC curves of acetonitrile adsorbed onto MCM-41 together with that of the bulk curve. Measurements were conducted in both cooling and heating directions at 5 K min^{-1}. When cooled, bulk acetonitrile gave two exothermic peaks, and when the temperature of the sample was increased after freezing, two endothermic peaks at temperatures higher than those in the former case were obtained. The first peak found in cooling is due to freezing of α-type acetonitrile for supercooled liquid acetonitrile and the second peak is due to the phase transition from α-type to β-type. The latter peak was not clearly seen and sometimes changed the spectral profile and/or did not appear. In the latter case, when heated after cooling, the exothermic peak appeared first and presented two endothermic peaks. This is because the phase transition from α-type to β-type is a very slow process. Thus, after observing the exothermic peak due to freezing, the sample was kept just below the freezing temperature for 1 h to increase

the exothermic peak. Hence, DSC analysis was conducted on the data observed at increasing temperatures.

When the acetonitrile was introduced into the pores of MCM-41, the temperatures of thermal changes were displaced significantly downward with decrease in pore size. The limiting pore size is 2.91 Å (C14) below which no phase transition has been observed. Endothermic peaks measured in the heating direction appeared at temperatures higher than those observed in the cooling direction: the former peaks are composed of two endothermic peaks. It is obvious that acetonitrile is supercooled also in the mesopores, similarly to that of bulk liquid. The endothermic peaks of these systems were reversibly determined and can be understood as describing the intrinsic temperature for the system. In the samples C18 and C22, the shapes of the peaks are apparently single ones but composed of shoulders when examined precisely. Thus, it is proposed that exactly the same phase changes occur between liquid, α-type, and β-type in the mesopores of MCM-41 as in the bulk. This phase transition was not discerned by Wallacher et al.[13] and Aksnes et al.[34] on the acetonitrile in the cpg, probably because of its pore size distribution.

The shift of phase equilibrium of solid (s)−liquid (l) and/or solid−solid in the cylindrical pores with pore size has traditionally been analyzed by the Gibbs−Thomson relation. If I−II change represents the phase change, and equilibrium is maintained with change in pore size:

$$dG_{II} - dG_I = 0 = -(\bar{S}_{II} - \bar{S}_I)dT - 2\left(\frac{\nu_{II}\gamma_{II}}{R_2} - \frac{\nu_I\gamma_I}{R_2}\right)dR \quad (1)$$

where $R = a - t$: a = intrinsic pore radius and t = thickness of the unfrozen layer at the interface. This relation has conventionally been simplified under the assumptions that molar volume change is negligible, i.e., $\upsilon_I = \upsilon_{II}$, and the enthalpy of phase change $\Delta\bar{H}$ does not vary with temperature and related with entropy change ($\Delta\bar{S} = \Delta\bar{H}/T$). Interfacial free energy values between the pore wall and internal matter do not vary with temperature. Then relation 2 is derived:

$$T_0 - T_R = \Delta T = -\frac{2\nu\Delta\gamma_{I-II}}{\Delta H_{II-I}R}T_0 \quad (2)$$

where T_0 is a melting point, and R the effective pore radius.

In Figure 6b, melting points and transition points are plotted as a function of inverse of effective radius ($1/R$), where R was varied by least-squares fitting between ΔT and $1/R$ so that the intersection point of the straight lines obtained agreed with the melting point and/or transition point of bulk matter. From this treatment, one can calculate the t value. The estimated t value was 0.7 nm, which is almost 1.40 times as large as that of the molecular diameter conventionally calculated from the density of liquid acetonitrile, $a = 0.498$ nm.[41] This allows for the surface roughness of the pores; that is, the surface is not homogeneous on an atomic scale with surface hydroxyls ca. 2.7 OH nm^{-2} and a siloxane part. In addition, molecular density varies markedly between the phases, 0.777 Mg m^{-3} for liquid acetonitrile (298 K), monoclinic (α-type) crystal 1.02 Mg m^{-3} (mp), and orthorhombic (β-type) 1.187 Mg m^{-3} (tp), respectively. Thus, the parameters obtained through relation 2 may present a measure of interfacial processes of condensed matters but also include important thermodynamic insight, since there are no other ways to estimate these parameters. Besides the thickness of the unfrozen layers, the slopes of the straight lines present interfacial energy changes for liquid/pore surface (ps) and α-type crystal/ps and for α-type/ps and β-type/ps: $\Delta\gamma_{(\alpha-l)} = 22.4$ mJ m^{-2} and $\Delta\gamma_{(\beta-\alpha)} = 3.17$ mJ m^{-2}, respectively. These values indicate the big difference in interfacial structures between liquid acetonitrile and α-type crystalline acetonitrile, and that between α-type and β-type acetonitriles.

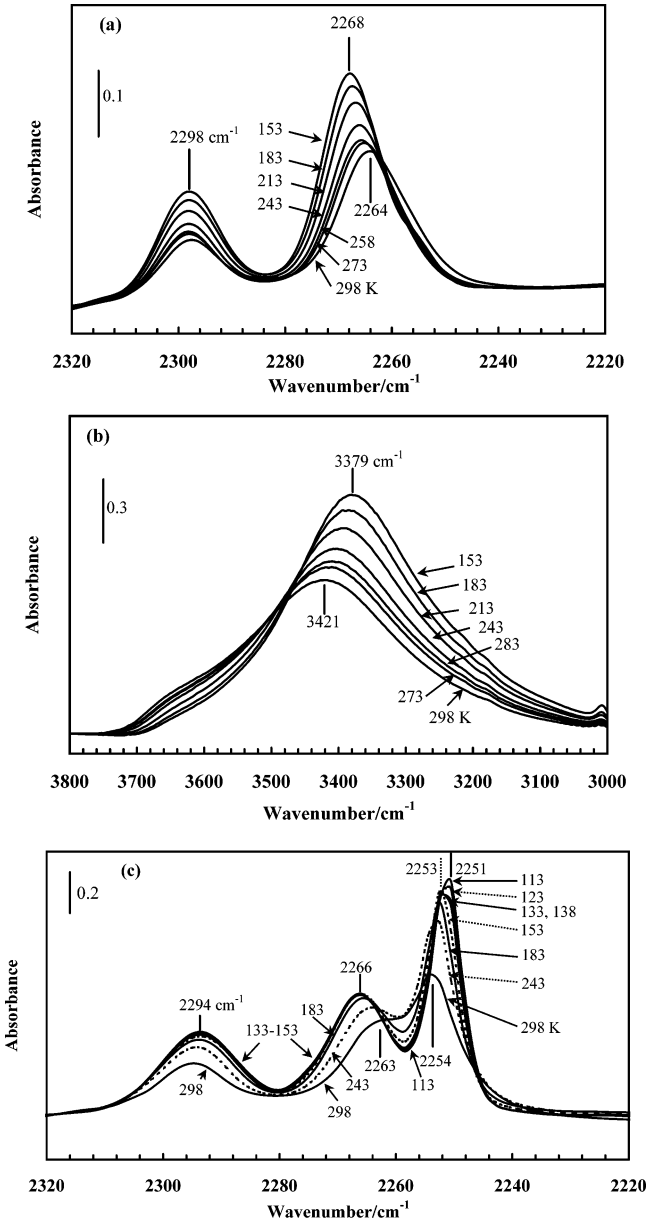

Figure 7. (a) Effect of temperatures on the FT-IR spectra of monolayer acetonitrile adsorbed on the C14 pore surface where adsorbed amount was adjusted at the relative pressure of 0.3 at 298 K. To avoid decay of adsorbed acetonitrile from pores, 1 atm nitrogen gas was introduced in the system. (b) Effect of temperatures on the FT-IR spectra of surface hydroxyls of the C14 pore surface where monolayer acetonitrile was adsorbed at the relative pressure of 0.3 at 298 K. (c) Effect of temperatures on the FT-IR spectra of acetonitrile capillary condensed into C14 where adsorbed amount was adjusted at the relative pressure of 0.7 at 298 K. 1 atm nitrogen gas was introduced in the system, as well. Measurement was conducted at increasing temperatures after freezing the system.

Phase Properties at Low Temperatures Observed by FT-IR Measurements. Figure 7a shows the effect of temperature on the FT-IR spectrum of monolayer acetonitrile. Lowering of the temperature displaces the 2264 cm^{-1} band slightly to higher wavenumbers together with an increase in peak height. When the pure acetonitrile was cooled, the absorption band

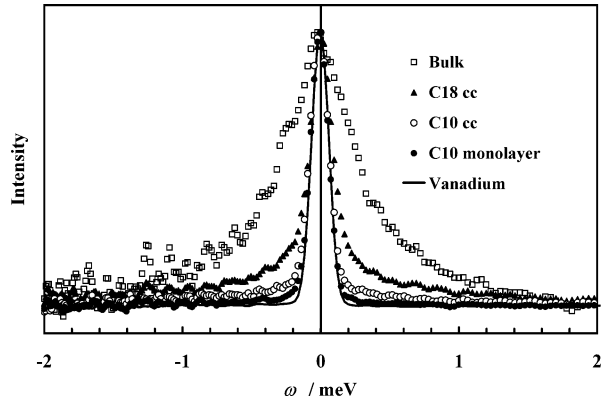

Figure 8. Comparison of quasi-elastic neutron scattering spectra of vanadium, liquid acetonitrile, acetonitrile capillary condensed in the C18 and C10 mesopores, and monolayer acetonitrile on the pore surface of C10, which have been determined at 297 K.

increased but did not change position at temperatures above freezing (Figure 5). Thus, this shift is related to the change in the adsorbed state of the acetonitriles interacting with surface hydroxyls. This is supported by the parallel displacement of OH bands from higher wavenumbers to lower wavenumbers with decrease in temperature (Figure 7b). This fact indicates that the hydrogen bond is strengthened by cooling. Ahn and Lee proposed through ab initio calculation using Gaussian 94 that when the hydrogen bond between water and acetonitrile ($H-O-H\cdots N\equiv C-CH_3$) is folded, the C≡N stretching band underwent a blue shift; i.e., it was displaced to higher wavenumbers.[42] Tanaka et al. have measured the temperature effect at rather higher temperature ranges 283−332 K and observed the decrease in peak position with temperature increase.[43] They calculated the decreasing correlation time of acetonitrile, suggesting the weakening of them. This fact must be substantiated by structure analysis using X-ray diffraction and/or neutron diffraction.

When the capillary condensed system is cooled, the 2263 cm^{-1} band is displaced to 2266 cm^{-1} (Figure 7c). On the other hand, the 2254 cm^{-1} band due to the central part of adsorbed acetonitrile in the capillary increases in intensity with slight change in the position down to 2253 cm^{-1} at 153 K, followed by apparent broadening to lower wavenumbers at 133 and 138 K. This agrees with the appearance of the endothermic peak at 141 K, i.e., melting of α-phase and phase transition of acetonitrile. Lowering of the temperature down to 123 and 113 K presents sharp band (2251 cm^{-1}) corresponding to the β-phase (Figure 6a). Thus, acetonitrile in the pore takes two clearly separated phases, monolayer and central phases.

Quasi-Elastic Neutron Scattering Spectra of Confined Acetonitrile. The effect of confinement on the dynamic properties of acetonitrile was studied by QENS measurements. Figure 8 shows QENS spectra of vanadium, bulk acetonitrile, and adsorbed acetonitrile on the pore surface (monolayer), and capillary condensed acetonitrile (cc). The spectrum of vanadium is purely ascribable to elastic scattering and its profile coincides with that of a dried MCM-41 sample (not shown) that had been used for obtaining net spectra of acetonitrile. It is clear that monolayer acetonitrile gives a very strong sharp peak and a small but definite sleeve at the foot of the spectrum, indicating that the monolayer acetonitrile is strongly solidified by surface forces. Some dynamic motion is not negligible. With capillary condensed systems line broadening is obvious and that for the sample C18 is more significant than for C10. The following analyses of the spectra were made on the net spectra, which were the differences between raw spectra observed with acetonitrile in the mesopores and those for dried samples. Parts a and b of Figure 9 show the spectral changes for bulk acetonitrile and capillary condensed acetonitrile in the C18 as a function of momentum transfer determined at 298 K. The line broadening of the spectrum for the bulk liquid is obvious and indicates that dynamic motion is very rapid. In the case in which acetonitrile is confined, one can clearly see the sharp peak at the center of the spectrum accompanied by a broadened sleeve. The presence of this peak shows that some of the neutrons are elastically scattered; i.e., there are acetonitrile molecules that do not have fast dynamic properties detectable by QENS.

These QENS spectra were analyzed as follows. Possible dynamic motions of acetonitriles are rotations around the molecular axis, tumbling rotational diffusion, and translational diffusion. Acetonitriles involved in the present system are monolayer molecules anchored to the surface hydroxyls and capillary condensed molecules located in the interior pore space. QENS peak intensity is proportional to the scattering law $S(Q,\omega)$ expressed by using component scattering laws of their contributions:

$$S(Q,\omega) = \exp\left(\frac{-Q^2\langle u^2\rangle}{3}\right)[AS_{\mathrm{ml}}(Q,\omega) + (1-A)S_{\mathrm{cc}}(Q,\omega)] + B \quad (3)$$

where the exponential term is the Debye−Waller factor, u is the vibration amplitude of the molecules, and A is the ratio of the number of monolayer molecules to total adsorbed molecules. $S_{\mathrm{cc}}(Q,\omega)$ is the scattering law of acetonitrile in the central part of the pore. B is the background intensity. In view of the rather less qualified nature of the spectra and limit of precision of the analytical methods, some assumptions were made. The contribution of the monolayer molecules, $S_{\mathrm{ml}}(Q,\omega)$, is ascribed to the rotational motion of methyl group, $S_{\mathrm{RMe}}(Q,\omega)$, which is involved in the scattering for cc- acetonitrile. A scattering law for the central part molecules $S_{\mathrm{cc}}(Q,\omega)$, eq 4, is expressed by convolution of (5) for rotation of methyl group, $S_{\mathrm{RMe}}(Q,\omega)$, molecular overall rotation $S_{\mathrm{R}}(Q,\omega)$, eq 6, and $S_{\mathrm{T}}(Q,\omega)$ for translational diffusion of acetonitrile molecules, eq 7:[44]

$$S_{\mathrm{cc}}(Q,\omega) = S_{\mathrm{RMe}}(Q,\omega) \otimes S_{\mathrm{R}}(Q,\omega) \otimes S_{\mathrm{T}}(Q,\omega) \quad (4)$$

$$S_{\mathrm{RMe}}(Q,\omega) = \frac{1}{\pi}\int_0^{\pi} J_0^{\,2}(Qa_{\mathrm{ME}}\sin\theta)\delta(\omega)d\theta \quad (5)$$

$$S_{\mathrm{R}}(Q,\omega) = J_0^{\,2}(Qa_{\mathrm{R}})\delta(\omega) + 3J_1^{\,2}(Qa_{\mathrm{R}})L(\omega,\Gamma_{\mathrm{R1}}) + 5J_2^{\,2}(Qa_{\mathrm{R}})L(\omega,\Gamma_{\mathrm{R2}}) \quad (6)$$

$$S_{\mathrm{T}}(Q,\omega) = L(\omega,\Gamma_{\mathrm{T}}) + \frac{1}{\pi}\frac{\Gamma_{\mathrm{T}}}{\omega^2+\Gamma_{\mathrm{T}}^{\,2}} \quad (7)$$

where J_{n} and j_n are Bessel and spherical Bessel functions, respectively. a_{Me} and a_{R} are the rotation radii of the methyl group (1.02 nm) and overall tumbling rotation of acetonitrile (1.95 nm), respectively.[45] Rotation of methyl group is described a uniaxial rotational diffusion model.[44] In the present analysis, we neglect quasi-elastic component of this model as shown in eq 5, because the rotation of the methyl group is so fast (typical relaxation time is 0.3−0.6 ps[45] that the quasi-elastic component is very broad and can be regarded as a flat baseline. $L(\omega,\Gamma_{\mathrm{R1}})$ and $L(\omega,\Gamma_{\mathrm{R2}})$ are Lorentzian functions for rotational motions.

TABLE 1: Dynamic Parameters of Bulk and Capillary Condensed Acetonitrile

samples	T/K	$D_T/10^{-10}$ m^2 s^{-1}	τ_R/ps	prop. of scattering intens of ML
bulk	297	33 ± 1	1.4 ± 0.2	
	260	17 ± 1	1.4 ± 0.1	
	235	9.1 ± 0.3	2.4 ± 0.2	
C18	297	9.9 ± 0.6	1.4 ± 0.3	0.11 ± 0.02
	260	4.9 ± 0.3	2.5 ± 0.1	0.18 ± 0.01
	235	4.7 ± 0.5	1.5 ± 0.3	0.09 ± 0.01
C10	297	2.7 ± 0.5	2.5 ± 0.3	0.36 ± 0.02

Here Γ_{R1} and Γ_{R2} (half-width at half-maximum, hwhm) are defined as follows

$$\Gamma_{R1} = \frac{1}{3\tau_R} \quad \text{and} \quad \Gamma_{R2} = \frac{1}{\tau_R} \tag{8}$$

where τ_R is the relaxation time for tumbling rotational motion.

For simplicity, the translational diffusion of the molecules was calculated by the traditional eq 9:

$$\Gamma_T = DQ^2 \tag{9}$$

Here, the fitting was conducted simultaneously on all of the spectra observed for each system using a modified Kiwi fitting program.[46]

All of the fitting parameters are shown in Table 1. In the last column, the ratios of monolayer acetonitriles determined by the QENS experiment are shown. The values are almost constant when temperature is decreased. The larger ratio for the C10 sample reflects the large amount of monolayer acetonitriles in the MCM-41 deduced by adsorption measurements (Figure 2), FT-IR measurements (Figure 4), and DSC data obeying the G−T relation.

The logarithms of translational diffusion coefficients D_T for the bulk and capillary condensed acetonitriles are plotted as a function of $1/T$ in Figure 10. The bulk values decrease monotonically with decrease in temperature. When introduced in the pores of MCM-41, the diffusion coefficient decreases with decrease in pore sizes. It is noted that the temperature effect is not significant in such a wide range, indicating the smaller activation energy of diffusion of acetonitriles in this temperature range, ~7 kJ mol^{-1}; for bulk liquid it is 12.1 kJ mol^{-1}. A similar confinement effect has been observed in systems with water and methanol in MCM-41.[46,47] In the case of water in C18 of MCM-41, activation energy was estimated to be 24 kJ mol^{-1} compared with bulk value of 20.2 kJ mol^{-1} around at room temperature; the latter increases at low temperatures due to enhancement of hydrogen bonding. With methanol, activation energies are 1.4 and 12.05 kJ mol^{-1} for acetonitrile in C-14 and for bulk liquid, respectively. These facts suggest that interaction of hydroxyls of water with surface hydroxyls is involved in the dynamic processes. As indicated by the interface energy effect on the melting point, the liquid itself remains fluidized at temperatures lower than the melting point of bulk matter. The molecules in a cylindrical pore have the possibility of diffusing freely along the direction of the cylinder, but are inhibited in the other direction. The apparently lowered diffusion coefficients suggest that some surface force inhibits the dynamic motion of the central liquid. FT-IR spectroscopy analysis (Figure 7b) shows that, when the system is cooled, a vibration mode of acetonitrile in the central part of the cylinder changes gradually to that of bulk acetonitrile, indicating the occurrence of a clearer separation of inner acetonitrile from monolayer acetonitrile. Furthermore, inner molecules become relatively less viscous at temperatures lower than those interacting with monolayer molecules. This explains the slow decrease in diffusion coefficient with temperature.

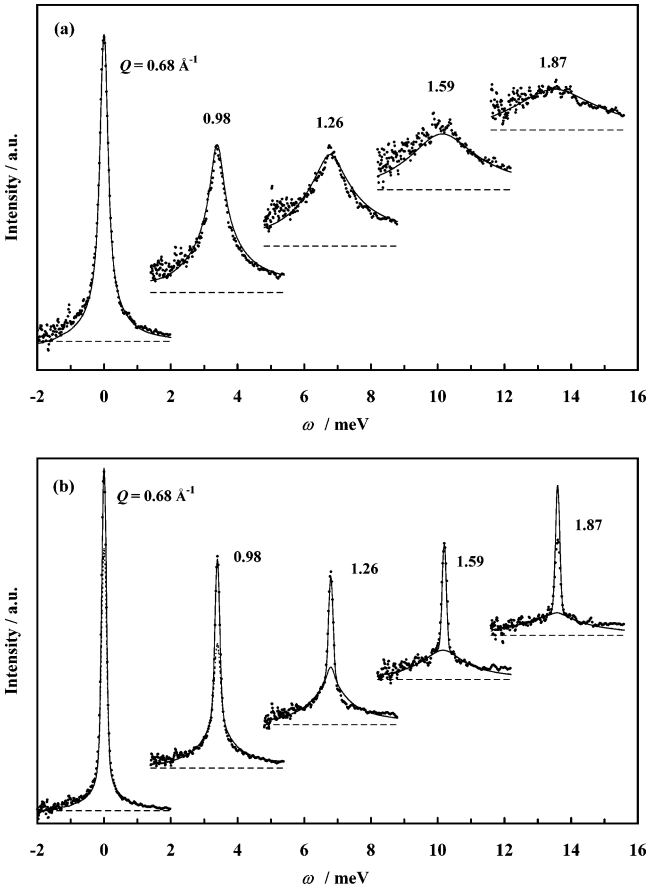

Figure 9. (a) QENS spectra of liquid acetonitrile as a function of moment transfer of neutrons. Solid lines are fitting curves according to the relations in the text. Broken lines are for baselines. (b) QENS spectra of acetonitrile capillary condensed in the C18. Dotted lines are fitted quasi-elastic part of scattering and solid ones are for total fitting data. Broken lines are for baselines

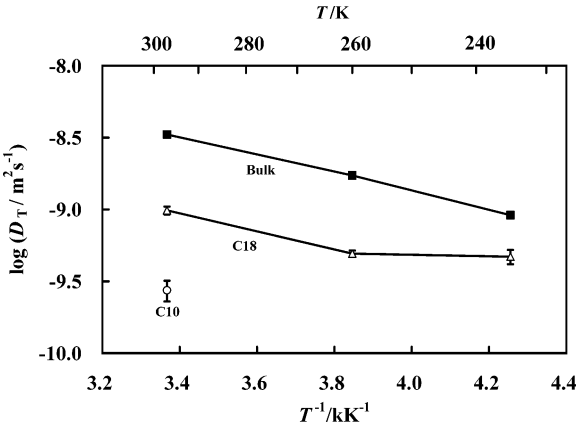

Figure 10. Dependence of translational diffusion coefficients of acetonitrile on the temperatures for bulk and capillary condensed molecules of C10 and C18.

Figure 11 shows the relaxation times of rotation of bulk and confined acetonitrile molecules. Tanaka et al. studied the rotational motions of acetonitrile in MCM-41 ($d = 3.2$ nm) by the analysis of line broadening of IR spectra of C≡N stretching vibrations and determined to be 1.7−18 ps at 303 K that was very similar to the bulk value of 1.7 ps at 298 K.[42] Effect of

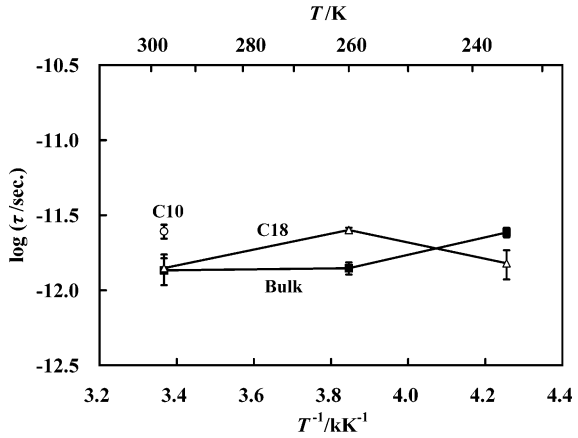

Figure 11. Dependence of relaxation times of rotational motion of acetonitrile on the temperature for bulk and capillary condensed acetonitrile of C10 and C18.

temperature is quite small. This is not an abnormal case and is often observed by QENS experiments on fluids.[14,48]

Conclusions

Acetonitrile molecules take two kinds of state in the mesopores of MCM-41, monolayer molecules that are anchored to surface hydroxyls by hydrogen bonding and capillary condensed central molecules second order capillary condensed). Thermodynamic measurement clearly distinguishes the two phases. Thermodynamic properties of acetonitriles in the central part are strongly affected by confinement in the mesopores of MCM-41 ($d = 2.91-4.19$ nm). The temperatures of phase changes for liquid $\rightarrow$ α-type crystal $\rightarrow$ β-type crystal decrease with pore size, obeying the Gibbs−Thomson relation. That is, the contribution of interfacial free energies between fluid and solid surface layers (monolayer molecular arrangements) to the capillary condensed acetonitrile is significant in deciding its phase. Acetonitrile molecules in the central part of pores below 2.91 nm are not frozen at the lowest temperatures measured. Translational motion of fluid acetonitrile in MCM-41 is restricted by confinement, but the temperature effect on lowering is slight because of the separation of inner molecules from monolayer part. Rotational motion, on the other hand, is not affected by confinement and is very similar to the bulk rotational motion.

Acknowledgment. The authors express sincere thanks to Processor Tsuyoshi Kajitani of Tohoku University for his helps in neutron scattering experiments. Financial aid is appreciated to a Special Grant for Cooperative Research Administered by Japan Private School Promotion Foundation, 13HK11.

References and Notes

(1) Rouquerol, F.; Rouquerol, J.; Sing, K. *Adsorption by powders and porous solids*; Academic Press: San Diego, CA, 1999.
(2) Christenson, H. K. *J. Phys.: Condens. Matter* **2001**, *13*, R95.
(3) Seki, K. *Adsorpt. News* **2004**, *18*, 6.
(4) Gelb, L. D.; Gubbins, K. E. *Stud. Surf. Sci. Catal.* **2000**, *128*, 61.
(5) Wolf, J.; Bryant, G.; Koster, K. L. *Cryo-Lett.* **2002**, *23*, 157.
(6) Ritter, M. *The Physical Environment: An Introduction of Physical Geology*; On line Textbook 2003.
(7) Gregg, S.; Sing, K. S. W. *Surface and Colloid Science*; Matijević, Egon, Ed.; John Wiley and Sons: New York, 1976; Vol. 9, p 231.
(8) Washburn, E. W. *Phys. Rev. Ser.* **1921**, *2*, 273.
(9) Yanagisawa, T.; Shimizu, T.; Kuroda, K.; Kato, C. *Bull. Chem. Soc. Jpn.* **1990**, *63*, 988.
(10) Kresge, C. T.; Leonowicz, M. E.; Roth, W. J.; Vartuili, J. C.; Beck, J. S. *Lett. Nature* **1992**, *359*, 710.
(11) Shao, D.; Huo, O.; Feng, J.; Chelka, B. F.; Stucky, G. D. *J. Am. Chem. Soc.* **1998**, *120*, 6024.
(12) Kruk, M.; Jaroniec, M.; Sakamoto, Y.; Terasaki, O.; Ryoo, R.; Ko, C. H. *J. Phys. Chem. B* **2000**, *104*, 292.
(13) Wallacher, D.; Soprunyuk, V. P.; Knorr, K.; Kityk, A. V. *Phys. Rev. B* **2004**, *69*, 134207.
(14) Bellissent Funel, M. C.; Chen, S. H.; Zanotti, J. M. *Phys. Rev. E* **1995**, *51*, 4558.
(15) Hellweg, T.; Schemmel, S.; Rother, G.; Brûlet, A.; Eckerlebe, H.; Findenegg, G. H. *Euro. Phys. E: Soft Matter* **2003**, *12*, 1.
(16) *J.* Loughnane, B. J.; Farrer, R. A.; Scodinu, A.; Reilly, T.; Fourkas, J. T. *J. Phys. Chem. B* **2000**, *104*, 5421.
(17) Akporiaye, D.; Hansen, E. W.; Schmidt, R.; Socker, M. *J. Phys. Chem.* **1994**, *98*, 1926.
(18) Hansen, W. E.; Schmidt, R.; Socker, M.; Akporiaye, D. *J. Phys. Chem.* **1995**, *99*, 4148.
(19) Inagaki, S.; Fukushima, Y.; Kuroda, K.; Kuroda, K. *J. Colloid Interface Sci.* **1996**, *180*, 623.
(20) Morishige, K.; Nobuoka, K. *J. Chem. Phys.* **1997**, *107*, 6965.
(21) Takahara, S.; Nakano, M.; Kittaka, S.; Kuroda, Y.; Mori, T.; Hamano, H.; Yamaguchi, T. *J. Phys. Chem.* **1999**, *103*, 5814.
(22) Rozwadowski, M.; Lezanska, M.; Wloch, J.; Erdmann, E.; Goleembiewski, R.; Kornatowski, J. *Langmuir* **2001**, 17, 2112.
(23) Schreiber, A.; Ketelsen, I.; Findenegg, G. H. *Phys. Chem. Chem. Phys.* **2001**, *3*, 1185.
(24) Faraone, A.; Liu, L.; Mou, C.-Y.; Yen, C.-W.; Chen, S.-H. *J. Chem. Phys.* **2004**, *121*, 10843.
(25) Liu, L.; Faraone, A.; Mou, C.-Y.; Yen, C.-W.; Chen, S.-H. *J. Phys.: Condens. Matter* **2004**, *16*, S5403.
(26) Tun, Z.; Mason, P. C. *Langmuir* **2002**, *18*, 975.
(27) Ribeiro Carrotto, M. M. L.; Estêvao Cadeias, A. J.; Carrot, P. J. M.; Unger, K. K. *Langmuir* **1999**, *15*, 8895.
(28) Mori, T.; Kuroda, Y.; Yoshikawa, Y.; Nagao, M.; Kittaka, S. *Langmuir* **2002**, *18*, 1595.
(29) Jackson, C. L.; McKenna, G. B. *J. Chem. Phys.* **1990**, *93*, 9002.
(30) Awschalom, D. D.; Warnock, J. "*Molecular Dynamics in Restricted Geometries*; Klafter, J., Drake, J. M., Eds.; Wiley: New York, 1989; Chapter 12.
(31) Rennie, G. K.; Clifford, J. *J. Chem. Soc. F1* **1977**, *73*, 680.
(32) Morishige, K.; Uematsu, H.; Tateishi, N. *J. Chem. Phys.* **2004**, *108*, 7241.
(33) Morterra, C.; Mentruit, M. P.; Cerrato, G. *Phys. Chem. Chem. Phys.* **2002**, *4*, 676.
(34) Aksnes, D. W.; Forland, K.; Kimtys, L. *Phys. Chem. Chem. Phys.* **2001**, *3*, 3203.
(35) Telkki, V. V.; Lounila, J.; Jokisaari, J. *J. Phys. Chem. B* **2005**, *109*, 757.
(36) Barrow, M. J. *Acta Crystallogr.* **1981**, *B37*, 2239.
(37) Antson, O. K.; Tilli, K. J.; Andersen, N. H. *Acta Crystallogr.* **1987**, *B43*, 296.
(38) Putnam, W. E.; McEachern Jr. D. M.; Kilpatrick, J. E. *J. Chem. Phys.* **1965**, *42*, 749.
(39) Machin, W. D. *Phys. Chem. Chem. Phys.* **2003**, *5*, 203.
(40) Tanaka, H.; Iiyama, T.; Uekawa, N.; Suzuki, T.; Matsumoto, A.; Grün, K. M.; Unger, K.; Katsumi, K. *Chem. Phys. Lett.* **1998**, *293*, 541.
(41) $a = 2(\pi M/8\rho A)^{1/3}$: ρ is the density of liquid molecule, M is molecular weight, and A is Avogadro's number.
(42) Ahn D. S.; Lee, S. *Bull. Korean Chem. Soc.* **2003**, *24*, 545.
(43) Tanaka, H.; Matsumoto, A.; Unger, K. K.; Kaneko, K. *Surf. Sci. Catal.* **2001**, *132*, 797.
(44) Bée, M. *Quasielastic Neutron Scattering*; Adam Hilger: Bristol, PA, and Philadelphia, PA, 1988; p 197.
(45) Böhm H. J.; McDonald, I. R. *Mol. Phys.* **1983**, *49*, 347.
(46) Takahara, S.; Kittaka, S.; Yamaguchi, T.; Bellissent-Funel, M.-C. *J. Phys. Chem.* B **2005**, *109*, 11231.
(47) Kittaka, S.; Serizawa, A.; Iwashita, T.; Takahara, S.; Takenaka, T.; Kuroda, Y.; Mori, T. *Surf. Sci. Catal.* **2001**, *132*, 653.
(48) Takahara, S.; Kittaka, S.; Mori, T.; Kuroda, Y.; Yamaguchi, T.; Bellissent-Funel, M.-C. *Adsorption* **2005**, *11*, 479.